ACS OMEGA

http://pubs.acs.org/journal/acsodf

Article

Comparison for Electron Donor Capability of Carbon-Bound Halogens in Tetrel Bonds

Qingqing Yang, Xiaolong Zhang,* and Qingzhong Li*

Cite This: *ACS Omega* 2021, 6, 29037−29044

Read Online

ACCESS | Metrics & More | Article Recommendations

ABSTRACT: The tetrel bond formed by HC≡CX, H_2C═CHX, and H_3CCH_2X (X═F, Cl, Br, I) as an electron donor and TH_3F (T═C, Si, Ge) was explored by ab initio calculations. The tetrel bond formed by H_3CCH_2X is the strongest, as high as −3.45 kcal/mol for the H_3CCH_2F···GeH_3F dimer, followed by H_2C═CHX, and the weakest bond is from HC≡CX, where the tetrel bond can be as small as −0.8 kcal/mol. The strength of the tetrel bond increases in the order of C < Si < Ge. For the H_3CCH_2X and HC≡CX complexes, the tetrel bond strength shows a similar increasing tendency with the decrease of the electronegativity of the halogen atom. Electrostatic interaction plays the largest role in the stronger tetrel bonds, while dispersion interaction makes an important contribution to the H_2C═CHX complexes.

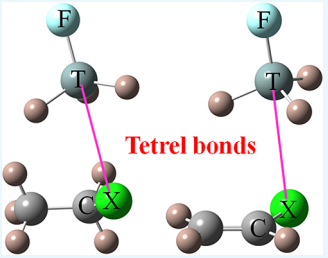

1. INTRODUCTION

The tetrel bond is an attractive interaction between a group 14 element and an electron donor.[1] Politzer and coauthors proposed a concept of σ-holes, referred to the electron-deficient outer lobe of a half-filled *p* orbital of a covalent bond, to explain the formation of a halogen bond.[2] Then, this concept was extended to other groups including the group 14 element (tetrel).[3] This σ-hole displays a region with positive molecular electrostatic potentials (MEPs) on the atomic surface along a covalent bond; thus, it can interact attractively with a negative site in another molecule. Subsequently, these authors named a π-hole to describe a region with positive MEPs that is vertical to a portion of a molecular framework.[4] Such a π-hole is also found for the group 14 element in sp^2-hybridized molecules. The presence of a σ-hole/π-hole indicates that the tetrel bond is electrostatically driven. Both the σ-hole and π-hole become larger going from the lighter to the heavier atoms in a given group of the periodic table; thus, it is expected that the tetrel bond becomes stronger. Other than electrostatic contributions, the stability of a tetrel-bonded complex is in part attributed to charge transfer from the electron donor to the acceptor.[5]

Like hydrogen and halogen bonds, the tetrel bond is of great importance in crystal materials,[1,6,7] chemical reactions,[5,8,9] molecular recognition,[10−12] and biological systems.[13−15] Therefore, there are lots of theoretical and experimental studies of tetrel bonds.[16−32] These applications are related to the directionality and strength of tetrel bond. Owing to the anisotropic distribution of electrostatic potentials and steric hindrance of a tetravalent tetrel atom,[23] the tetrel bond is sensitive to angular distortions, displaying directionality. Both the electron-donating substituents in the electron donor and the electron-withdrawing groups in the tetrel donor have an enhancing effect on the strength of the tetrel bond.[16−22] Sometimes, some unexpected substitution effects are found for tetrel bonds. For example, adding a $-CH_3$ group in formamidine could greatly increase the interaction energy of the SiH_3F complex from 60 to 80 kJ/mol.[21] Cooperativity can also strengthen or weaken tetrel bonds, and this effect plays an important role in constructing crystal materials.[24−32] Experimental and theoretical studies show that a tetrel bond is concurrent with an agostic Pb···H−C interaction in *N*′-(phenyl(pyridin-2-yl)methylene) isonicotinohydrazide−PbX complexes (X═Cl, I, NCS, NO_2).[30]

The electron donor in the tetrel bond is varied from neutral molecules with lone pairs and anions[33] to molecules with π electrons,[34] metal hydrides,[35] radicals,[36] and carbenes.[37] Even so, the electron donors used in studying tetrel bonds are usually from neutral molecules with lone pairs and anions. These molecules are often nitrogen/oxygen-containing,[38−51] partly because some of these complexes such as SiF_4···NH_3 and SiF_4···$N(CH_3)_3$ were identified experimentally.[38] The N hybridization in the nitrogen electron donor affects the tetrel bond, becoming stronger in the sp < sp^2 < sp^3 sequence.[39,40] When the carbonyl oxygen atom of malondialdehyde engages in a π-hole tetrel bond with F_2SiO, the intramolecular hydrogen bond is enhanced with proton transfer within this H bond.[46] NH_3 is inclined to form a H bond with the $-CF_3$ group adjoined to pyridine; however, the protonation on the nitrogen atom of pyridine promotes the formation of a tetrel

Received: July 31, 2021
Accepted: October 14, 2021
Published: October 22, 2021

https://doi.org/10.1021/acsomega.1c04085
ACS Omega 2021, 6, 29037−29044

bond.[49] Dong and coauthors compared σ−/π-hole tetrel bonds between TH_3F/F_2TO and H_2CX (X═O, S, Se) and found an interesting dependence of their strengths on the chalcogen electron donor.[51] The σ-hole interaction is weaker for the heavier chalcogen electron donor, while the π-hole interaction involving F_2TO (T═Ge, Sn, and Pb) has an opposite dependence.[51]

Halogen anions have been used in studying tetrel bonds since they can be utilized in molecular recognition.[52−54] Regardless of which receptors (hydrogen, halogen, chalcogen, pnicogen, and tetrel), F^- is bound much more strongly than Cl^- and Br^-.[53] More surprisingly, the tetrel receptor shows the greatest selectivity for F^- over the other halides, as much as 10^{13}, an enhancement of six orders of magnitude when compared to the H-bonding receptor.[53] Likely, the halogen anion in LiX forms a stronger tetrel bond than neutral molecules and the tetrel bond becomes weaker for the heavier halogen ion.[55] The ionic property of HArF makes the negatively charged F atom become a good electron donor in the tetrel bond.[56] The tetrel bonding interaction energy between HArF and SiH_3X (X = halogen) is in a range of 95−135 kJ/mol at the MP2/CBS level.[56] Interestingly, the interaction energy becomes larger with the increase of X atomic mass in SiH_3X although the heavier X atom shrinks the σ-hole on the Si atom.[56] However, hydrogen halides are seldom used as the electron donors in tetrel bonds.[57,58] In the ground-state geometry, CO_2 forms a hydrogen bond with HCl but a tetrel bond with HBr in which the negatively charged Br atom approaches the carbon atom of CO_2.[57] SiH_4, SiF_4, and $SiCl_4$ bind with NH_3 through a tetrel bond, but they form a hydrogen bond with HF where the hydrogen atom interacts with the silicon substituents.[58] It was demonstrated that organic fluorine molecules have been extensively utilized in crystal engineering and functional materials.[59] However, the study of tetrel bonds involving organofluorine electron donors is sporadic.[60,61] CH_3F forms a weaker tetrel bond with SiH_3X (X═F and Cl) than NH_3.[60] There is evidence for the C−F···C═O π-hole tetrel bond in protein−drug interaction although its interaction energy is less than 5 kJ/mol.[61]

In this manuscript, we focus on the tetrel bond between TH_3F (T═C, Si, Ge) and organic fluorine electron donors. The organic fluorine molecules studied contain CH_3CH_2F (sp^3), CH_2CHF (sp^2), and CHCHF (sp). Then, the F atom in the organic fluorine is replaced by Cl, Br, and I. We systematically study the tetrel bond involving organic halogen electron donors. Can these organic halogens form a stable tetrel-bonded complex? How does the strength of tetrel bond depend on the nature of tetrel and halogen? What is the dominant origin of the tetrel bond? These tetrel bonds are characterized by means of geometries, energetics, natural bond orbital (NBO), atoms in molecules (AIM), and energy decomposition (EDA) analyses.

2. COMPUTATIONAL METHODS

The geometries of monomers and binary complexes were optimized at the MP2/aug-cc-pVTZ level. In addition, in order to consider the relativistic effects, the aug-cc-pVTZ-PP basis set was used for the I atom. Harmonic frequency calculations were performed at the same level to verify that the structures are local minima on their respective potential energy surfaces. The full counterpoise procedure was employed to correct for the basis set superposition error (BSSE).[62] All calculations were carried out using the Gaussian 09 package.[63]

The molecular electrostatic potentials (MEPs) of the monomers on the 0.001 a.u. isodensity surface were evaluated at the MP2/aug-cc-pVTZ level using the Wave Function Analysis-Surface Analysis Suite (WFA-SAS) program.[64] Natural bond orbital (NBO)[65] analysis was performed at the HF/aug-cc-pVTZ level to obtain orbital interaction and charge transfer (CT). The AIM2000 software[66] was carried out to obtain the electron density (ρ), energy density (H), and Laplacian ($\nabla^2\rho$) at the relevant bond critical points (BCPs). The LMOEDA[67] (localization molecular orbital energy decomposition analysis) was performed at the MP2/aug-cc-pVTZ level using the GAMESS program.[68] According to LMOEDA, the total interaction energy of a complex was decomposed into electrostatic energy (E^{ele}), exchange energy (E^{ex}), repulsion energy (E^{rep}), polarization energy (E^{pol}), and dispersion energy (E^{disp}).

3. RESULTS

3.1. MEP Analysis. The MEP maps of TH_3F (T═C, Si, Ge) monomers are shown in Figure 1. As indicated in Figure 1,

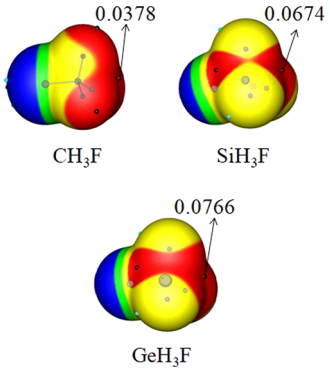

Figure 1. MEP maps of CH_3F, SiH_3F, and GeH_3F on the ρ = 0.001 a.u. isodensity surface. Color ranges, in a.u., are: red, greater than 0.02; yellow, between 0.02 and 0; green, between 0 and −0.02; and blue, smaller than −0.02.

Table 1. Most Negative MEP (V_{min}, a.u.) on the X (X═F, Cl, Br, I) Atomic Surface in the Monomers

	n = 1	n = 2	n = 3
Csp^n-F	−0.0064	−0.0318	−0.0456
Csp^n-Cl	−0.0046	−0.0208	−0.0287
Csp^n-Br	−0.0055	−0.0198	−0.0265
Csp^n-I	−0.0056	−0.0177	−0.0213

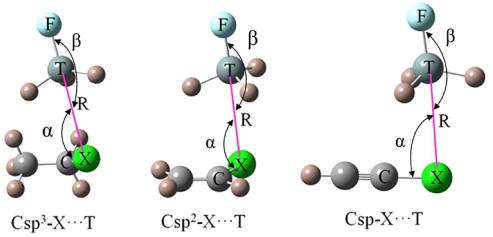

Figure 2. Schematic diagrams of three complexes.

all TH_3F monomers possess a region with positive MEPs (σ-hole) along the extension of the T−F bond. The increase of MEP on the σ-hole follows the order of C < Si < Ge, and the maximum value of GeH_3F is 0.0766 a.u. According to our

https://doi.org/10.1021/acsomega.1c04085
ACS Omega 2021, 6, 29037−29044

Table 2. Binding Distance (R, Å), Angles of C−X···T (α, °) (X═F, Cl, Br, I; T═C, Si, Ge) and X···T−F (β, °) in Complexes

	n = 1			n = 2			n = 3		
complexes	R	α	β	R	α	β	R	α	β
Csp^n-F···C	3.163	92.6	177.3	3.019	106.6	176.0	2.963	106.3	175.6
Csp^n-F···Si	3.120	103.8	176.4	2.925	110.1	178.7	2.793	113.9	179.6
Csp^n-F···Ge	3.098	100.8	173.8	2.871	110.5	178.2	2.754	110.5	177.7
Csp^n-Cl···C	3.547	78.3	172.4	3.434	87.9	170.3	3.401	84.8	168.4
Csp^n-Cl···Si	3.440	85.4	176.5	3.325	88.8	176.7	3.262	91.9	177.3
Csp^n-Cl···Ge	3.435	82.6	175.0	3.301	87.7	175.7	3.239	88.9	175.2
Csp^n-Br···C	3.561	76.6	174.3	3.501	83.6	168.9	3.478	80.3	167.9
Csp^n-Br···Si	3.496	82.2	176.4	3.407	84.1	176.1	3.358	87.2	176.6
Csp^n-Br···Ge	3.567	76.1	176.7	3.404	82.6	174.9	3.355	84.3	174.6
Csp^n-I···C	3.728	72.0	173.5	3.706	76.2	162.8	3.682	73.8	162.8
Csp^n-I···Si	3.679	76.9	175.0	3.604	78.4	174.7	3.567	80.9	175.1
Csp^n-I···Ge	3.702	73.8	173.6	3.613	76.9	173.3	3.572	78.1	173.4

Table 3. Interaction Energy (E_{int}, kcal/mol) in Complexes

complexes	n = 1	n = 2	n = 3
Csp^n-F···C	−0.80	−1.40	−1.67
Csp^n-F···Si	−0.97	−2.27	−3.20
Csp^n-F···Ge	−1.02	−2.53	−3.45
Csp^n-Cl···C	−1.25	−1.61	−1.56
Csp^n-Cl···Si	−1.69	−2.61	−3.05
Csp^n-Cl···Ge	−1.86	−2.88	−3.24
Csp^n-Br···C	−1.35	−1.60	−1.56
Csp^n-Br···Si	−1.79	−2.26	−3.01
Csp^n-Br···Ge	−1.98	−2.90	−3.17
Csp^n-I···C	−1.38	−1.60	−1.53
Csp^n-I···Si	−1.86	−2.57	−2.87
Csp^n-I···Ge	−2.10	−2.87	−3.04

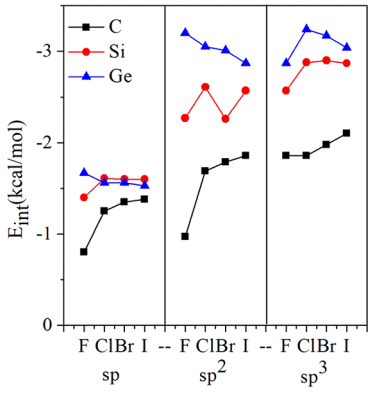

Figure 3. Dependence of interaction energy (E_{int}) on the nature of X and T atoms.

previous studies, the MEP distribution of CHCF exhibits a negative region on the F end.[69] Thus, the σ-hole of TH_3F monomer can form a weak tetrel bond with the most negative MEP region of CHCX (X═F, Cl, Br, I). In addition, the π-electrons in CH_2CHX and CHCHX also participate in a tetrel bond with TH_3F.[34]

Table 1 lists the most negative MEP value V_{min} of all Lewis bases. The minimum value is only −0.0046 a.u. When the halogen atom is fixed, due to the difference in the electron donating ability of different hybridization types C, the negative MEP value decreases according to Csp^3-X > Csp^2-X > Csp-X. When the hybrid type is the same, the most negative MEP in Csp^n-X (n = 2, 3) molecules gradually decreases in the order of

Table 4. Charge Transfer (CT, e) and NBO Perturbation Energy ($E^{(2)}$, kcal/mol) for Transfer from the X (X═F, Cl, Br, I) Lone Pair to the T−F (T═C, Si, Ge) Unfilled Antibonding Orbital

	n = 1		n = 2		n = 3	
complexes	CT	E$^{(2)}$	CT	E$^{(2)}$	CT	E$^{(2)}$
Csp^n-F···C	0.0006	0.19	0.0026	0.32	0.0003	0.57
Csp^n-F···Si	0.0038	0.56	0.0080	1.18	0.0112	2.74
Csp^n-F···Ge	0.0038	0.71	0.0094	1.67	0.0134	3.86
Csp^n-Cl···C	0.0018	0.33	0.0030	0.54	0.0021	0.81
Csp^n-Cl···Si	0.0084	1.60	0.0138	2.66	0.0181	4.05
Csp^n-Cl···Ge	0.0087	1.84	0.0156	3.41	0.0202	5.12
Csp^n-Br···C	0.0024	0.57	0.0036	0.72	0.0038	1.03
Csp^n-Br···Si	0.0122	2.36	0.0186	3.54	0.0234	4.94
Csp^n-Br···Ge	0.0127	2.72	0.0199	4.34	0.0259	5.97
Csp^n-I···C	0.0027	0.68	0.0033	0.73	0.0039	1.02
Csp^n-I···Si	0.0145	2.76	0.0208	3.84	0.0260	5.00
Csp^n-I···Ge	0.0140	2.96	0.0218	4.54	0.0272	5.88

F > Cl > Br > I, which is in agreement with the electronegativity trend observed for halogens. However, this is abnormal for Csp-X. The most negative electrostatic potential law is F > I > Br > Cl, probably because of the hyperconjugation effect between the π orbital on the C≡C bond and the lone pair on the halogen atom.

3.2. Energetics and Geometries. Figure 2 shows the geometries of complexes between Csp^n-X and TH_3F (X═F, Cl, Br, I; T═C, Si, Ge). For simplicity, CH_3CH_2X (sp^3), CH_2CHX (sp^2), and CHCHX (sp) are represented as Csp^3-X, Csp^2-X, and Csp-X, respectively, while TH_3F is denoted as T. As shown in Figure 2, R is the distance between the X atom in Csp^n-X and the T atom in TH_3F, and the related geometrical parameters are summarized in Table 2. For the sp-hybridized CHCX structures, the C−X···T (α) angle varies between 69 and 104° and is largest in the Csp-F system. This may be partly due to the coulomb attraction between the C≡C π electrons in Csp-X and the positive MEP near the H atoms in TH_3F, which is the weakest in the Csp-F system owing to the strongest electron-withdrawing ability of the F atom.

With the increasing X electronegativity, the α (C−X···T) angles for both sp^2 and sp^3 cases are increased in the same order of I < Br < Cl < F. Compared with the sp hybridization, the α (C−X···T) angle increases 1−40° for the sp^2 hybridization and 5−40° for the sp^3 hybridization, respectively. However, the β (X···T−F) angles for the three types of

https://doi.org/10.1021/acsomega.1c04085
ACS Omega 2021, 6, 29037−29044

Table 5. Electron Density (ρ), its Laplacian ($\nabla^2\rho$), and Total Energy Density (H) at the X···T BCP in Complexes (All in a.u.)

	n = 1			n = 2			n = 3		
complexes	ρ	$\nabla^2\rho$	H	ρ	$\nabla^2\rho$	H	ρ	$\nabla^2\rho$	H
Csp^n-F···C	0.0036	0.0219	0.0013	0.0052	0.0287	0.0015	0.0056	0.0331	0.0018
Csp^n-F···Si	0.0054	0.0243	0.0011	0.0080	0.0332	0.0011	0.0103	0.0399	0.0010
Csp^n-F···Ge	0.0061	0.0266	0.0011	0.0094	0.0399	0.0014	0.0121	0.0507	0.0016
Csp^n-Cl···C	0.0042	0.0209	0.0013	0.0043	0.0210	0.0013	0.0055	0.0242	0.0013
Csp^n-Cl···Si	0.0063	0.0231	0.0011	0.0080	0.0270	0.0010	0.0092	0.0289	0.0009
Csp^n-Cl···Ge	0.0066	0.0242	0.0011	0.0088	0.0299	0.0011	0.0103	0.0317	0.0010
Csp^n-Br···C	0.0049	0.0224	0.0013	0.0061	0.0242	0.0012	0.0063	0.0257	0.0013
Csp^n-Br···Si	0.0071	0.0236	0.0009	0.0079	0.0246	0.0007	0.0098	0.0276	0.0007
Csp^n-Br···Ge	0.0073	0.0241	0.0009	0.0092	0.0280	0.0008	0.0104	0.0290	0.0007
Csp^n-I···C	0.0053	0.0210	0.0011	0.0063	0.0221	0.0010	0.0065	0.0224	0.0010
Csp^n-I···Si	0.0074	0.0212	0.0006	0.0087	0.0233	0.0005	0.0096	0.0239	0.0004
Csp^n-I···Ge	0.0073	0.0210	0.0007	0.0088	0.0234	0.0005	0.0100	0.0241	0.0004

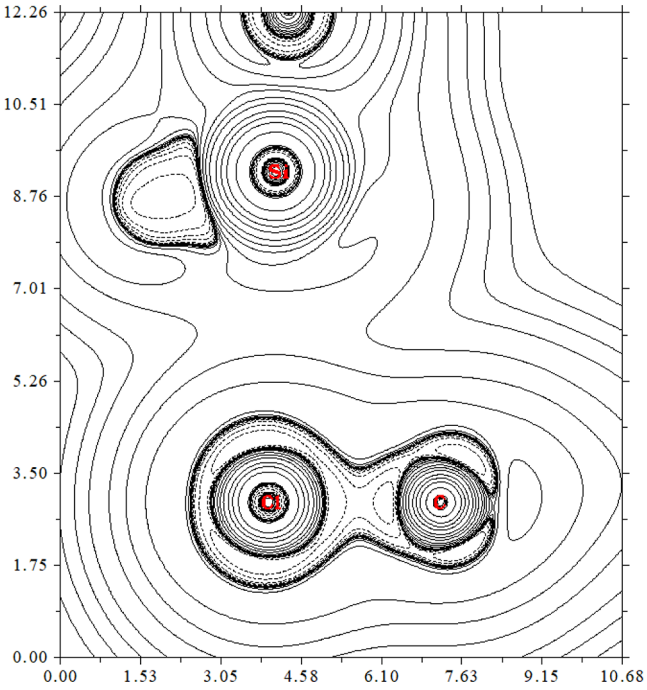

Figure 4. Laplacian contour of CH_2═CHCl···SiH_3F.

hybridizations are almost in the similar range from 163 to 180°, which is basically close to 180°.

When the TH_3F monomer is combined with the sp^2-hybridized H_2C═CHF, the TH_3F molecule is located above the plane of the olefin molecule. The corresponding intermolecular distance R (0.02−0.227 Å) is shorter than that in the sp hybridization. However, for the sp^3 hybridization, the intermolecular distance R is 0.01−0.116 Å, shorter than that in the sp^2 case. Clearly, the C hybridization has an obvious effect on the intermolecular distance. As one might expect, this bond contraction is accompanied by a very significant strengthening of the tetrel bond.

Table 3 lists the BSSE-corrected interaction energies of the binary complexes. As is evident from Table 3, for the sp hybridization, the interaction energies (absolute values) are increased in the order of C < Si < Ge, which are the same as those of the sp^2 and sp^3 cases. For a given R substitution, the order of the interaction energies (absolute values) is increased with sp < sp^2 < sp^3. When the C atom hybridization changes from sp to sp^2 and to sp^3, the negative MEP on the connected halogen atom gradually becomes larger (can be seen from the data in Table 1), so the tetrel bond formed by it becomes stronger. The shortest intermolecular distance R (2.755 Å) for the Csp^3-F···Ge complex has the largest E_{int} (−3.45 kcal/mol). However, there are some different trends for Csp-I···C, Csp-I···Si, and Csp-I···Ge complexes, i.e., R increases in the order of Si < Ge < C, while the E_{int} is C < Si < Ge. These tetrel bonds are much weaker than the charge-assisted tetrel bonds with the interaction energy larger than −16 kcal/mol.[54] Considering the small interaction energy, we think that these tetrel-bonded complexes are not stable at 298 K.

Figure 3 presents the relationship between the interaction energy E_{int} and the halogen substituents in different hybridization modes. For T═C complexes, the interaction energy shows a similar increasing tendency with the decrease of the electronegativity of halogen substituents. This is also the same for T═Si complexes in both sp and sp^3 hybridization except for sp^2 hybridization. However, for T═Ge complexes, the interaction energy decreases in the order of F < Cl < Br < I for both sp and sp^2 hybridization. On the other hand, for sp^3 hybridization, some inconsistent variations are found, i.e., for the X═Cl substituent, which exhibits the largest interaction energy.

3.3. NBO Analysis. We have performed the NBO calculations to study the nature of interaction. The results of the charge transfer and the second-order stabilization energies $E^{(2)}$ are gathered in Table 4. CT refers to the total amount of charge transfer from Csp^n-X to TH_3F, while $E^{(2)}$ focuses on the specific orbital transfer from Lp_X to $\sigma^*_{T\text{-}F}$ (Lp_X is the lone pair of electrons of halogen atoms and $\sigma^*_{T\text{-}F}$ is the antibonding orbital of the T-F bond). The charge transfer leads to the better understanding of the energetics: the largest for Ge and smallest for C, and it decreases with the increase of electronegativity X. From Table 4, for different hybridization, the value of CT increases significantly from sp to sp^2 to sp^3. The charge transfer of sp^2 hybridization varies from a low of 0.0026e to as much as 0.0218e. Those quantities represent an 18−77% enhancement relative to the sp complexes. However, the charge transfer of sp^3 hybridization is even twice that of sp.

In order to further analyze the nature of the orbital interaction, we have studied the second-order perturbation energy corresponding to the orbital interaction, and its value is estimated to in the range of 0.18−5.88 kcal/mol for all the complexes. When the X atom is the same, the $E^{(2)}$ of the Csp^n-X···T complex increases in the order of C < Si < Ge. The $E^{(2)}$ of the Csp^n-X···T complex increases in the order of F < Cl < Br

https://doi.org/10.1021/acsomega.1c04085
ACS Omega 2021, 6, 29037−29044

Table 6. Electrostatic (E^{ele}), Exchange (E^{ex}), Repulsion (E^{rep}), Polarization (E^{pol}), and Dispersion (E^{disp}) Energies in Complexes (All in kcal/mol)

complexes	E^{ele}	E^{ex}	E^{rep}	E^{pol}	E^{disp}
Csp-F···C	−0.47(22%)	−2.02	3.34	−0.15(7%)	−1.52(71%)
Csp-F···Si	−0.74(25%)	−2.92	4.91	−0.30(10%)	−1.95(65%)
Csp-F···Ge	−0.96(26%)	−3.73	6.32	−0.43(12%)	−2.24(62%)
Csp-Cl···C	−0.95(28%)	−3.26	5.32	−0.25(7%)	−2.17(64%)
Csp-Cl···Si	−1.45(27%)	−5.76	9.40	−0.74(14%)	−3.23(60%)
Csp-Cl···Ge	−1.76(28%)	−6.63	10.95	−0.91(15%)	−3.56(57%)
Csp-Br···C	−1.21(30%)	−4.24	6.94	−0.33(8%)	−2.52(62%)
Csp-Br···Si	−1.99(29%)	−7.69	12.62	−1.04(15%)	−3.76(55%)
Csp-Br···Ge	−2.29(30%)	−8.34	13.84	−1.18(16%)	−4.04(54%)
Csp-I···C	−1.47(31%)	−5.28	8.65	−0.43(9%)	−2.85(60%)
Csp-I···Si	−2.40(30%)	−9.46	15.51	−1.33(17%)	−4.21(53%)
Csp-I···Ge	−2.63(31%)	−9.73	16.14	−1.42(17%)	−4.48(53%)
Csp^2-F···C	−1.44(45%)	−2.76	4.58	−0.25(8%)	−1.54(48%)
Csp^2-F···Si	−3.06(48%)	−5.83	9.84	−0.81(13%)	−2.46(39%)
Csp^2-F···Ge	−4.07(52%)	−7.43	12.75	−1.13(14%)	−2.67(34%)
Csp^2-Cl···C	−1.09(41%)	−2.20	3.58	−0.21(8%)	−1.35(51%)
Csp^2-Cl···Si	−3.29(39%)	−8.93	14.66	−1.28(15%)	−3.88(46%)
Csp^2-Cl···Ge	−4.11(42%)	−10.44	17.41	−1.58(16%)	−4.21(43%)
Csp^2-Br···C	−1.92(38%)	−5.35	8.79	−0.47(9%)	−2.66(53%)
Csp^2-Br···Si	−3.35(39%)	−9.46	15.62	−1.39(16%)	−3.76(44%)
Csp^2-Br···Ge	−4.60(41%)	−12.31	20.59	−1.88(17%)	−4.73(42%)
Csp^2-I···C	−2.13(37%)	−6.50	10.68	−0.57(10%)	−3.04(53%)
Csp^2-I···Si	−4.10(38%)	−12.88	21.19	−1.90(17%)	−4.92(45%)
Csp^2-I···Ge	−4.69(39%)	−13.54	22.61	−2.07(17%)	−5.19(43%)
Csp^3-F···C	−1.76(53%)	−2.46	4.11	−0.30(9%)	−1.26(38%)
Csp^3-F···Si	−5.04(54%)	−8.50	14.58	−1.50(16%)	−2.81(30%)
Csp^3-F···Ge	−6.52(56%)	−11.03	19.18	−1.96(17%)	−3.15(27%)
Csp^3-Cl···C	−1.46(35%)	−4.13	6.76	−0.41(10%)	−2.33(55%)
Csp^3-Cl···Si	−4.43(43%)	−10.64	17.68	−1.68(16%)	−4.09(40%)
Csp^3-Cl···Ge	−5.70(46%)	−13.27	22.47	−2.14(17%)	−4.65(37%)
Csp^3-Br···C	−1.75(34%)	−5.53	9.08	−0.54(11%)	−2.81(55%)
Csp^3-Br···Si	−4.99(43%)	−12.86	21.41	−2.04(18%)	−4.62(40%)
Csp^3-Br···Ge	−6.07(45%)	−14.95	25.33	−2.40(18%)	−5.10(38%)
Csp^3-I···C	−1.93(33%)	−6.68	10.98	−0.65(11%)	−3.19(55%)
Csp^3-I···Si	−5.17(41%)	−14.58	24.22	−2.29(18%)	−5.09(41%)
Csp^3-I···Ge	−6.01(43%)	−16.03	27.10	−2.56(18%)	−5.55(39%)

< I for the same T atom, which is consistent with the change order of charge transfer CT. However, the largest amount of charge transfer does not necessarily correspond to the strongest bond. For example, Csp^n-I···Ge has the largest charge transfer, but the interaction energy is not the largest.

3.4. AIM Analysis. The electron density (ρ), its Laplacian ($\nabla^2\rho$), and energy density (H) at the bond critical point between X and T are listed in Table 5. All Csp^n-X···T interactions are characterized by a positive $\nabla^2\rho$ value and a positive H, which are indicative of a closed-shell interaction in these systems. The electron density exhibits the relationship with the X···T binding distance. One can see, the capacity of the complex to concentrate electrons increases as T═C < Si < Ge and X═F < Cl < Br < I, which is consistent with the tetrel bond distance as discussed above. In addition, for the different C hybridizations, the electron density is increased in the order of sp < sp^2 < sp^3. This has good agreement with the interaction energy discussed above. The electron density of the complexes is much less than 0.01 a.u., which means that the tetrel bond formed is a weak interaction. The Laplacian contour of CH_2═CHCl···SiH_3F is plotted in Figure 4, where the spatial display of Laplacian of electron densities is confined separately to both molecules, indicative of a weak closed-shell interaction.

3.5. EDA Analysis. To deepen the understanding of the nature of the tetrel bond, we performed an energy decomposition analysis for these complexes. The interaction energies were decomposed into electrostatic energy (E^{ele}), exchange energy (E^{ex}), repulsion energy (E^{rep}), polarization energy (E^{pol}), and dispersion energy (E^{disp}), which are collected in Table 6. This energy decomposition was performed with the GAMESS program and its energy terms have some different physical meanings from other energy decomposition schemes. The physical meanings of five terms obtained with the GAMESS program have been elaborated in the previous study;[67] thus, they are not described here. E^{ex} and E^{rep} are the largest attractive and repulsive terms, respectively, but both terms are dependent and partly cancel each other; thus, they are not discussed. As shown in Table 6, among three attractive terms (E^{ele}, E^{pol}, and E^{disp}), the contribution of E^{disp} to the stability of tetrel-bonded complexes is greater than the E^{ele} for the sp hybridization, while the E^{pol} has the smallest contribution. In addition, these five kinds of energies are increased in the order of sp < sp^2 < sp^3. This also shows good

https://doi.org/10.1021/acsomega.1c04085
ACS Omega 2021, 6, 29037−29044

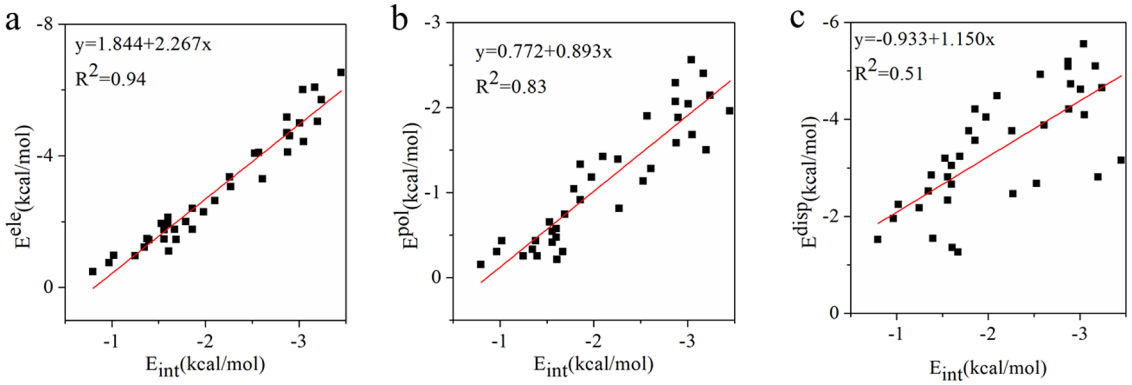

Figure 5. Relationship of interaction energy (E_{int}) with (a) electrostatic (E^{ele}), (b) polarization (E^{pol}), and (c) dispersion energies (E^{disp}).

agreement with the interaction energy discussed above. For the sp^2 hybridization, both E^{ele} and E^{disp} have similar degrees of magnitude, except for the Csp^2-F···Ge complex. This suggests that both terms make comparable contributions to the energetic stability of sp^2 complexes. For the sp^3 hybridization, the percentage for the E^{ele} contribution is 41−56% (except for Csp^3-X···C, X═Cl, Br, I), which means the E^{ele} term plays a dominant role in the energetic stability of most sp^3 complexes.

4. DISCUSSION

As discussed above for each type of C hybridization, the electrostatic and dispersion energies roughly reflect the behavior of the interaction energy. Figure 5a shows the linear relationship between E_{int} and E^{ele} for all complexes, with a correlation coefficient R^2 = 0.95. In addition, the slope in Figure 5a is 2.3, which indicates that the electrostatic energy increases faster than the interaction energy, while the slope is much closer to the dispersion energy in Figure 5c. Although dispersion energy plays an important role in the total interaction energy, its correlation with E_{int} is very poor, with R^2 = 0.53. In contrast, the correlation between E_{int} and E^{pol} is not very poor, with R^2 = 0.84 as indicated in Figure 5b.

The total amount of charge from the electron donor to the acceptor is less than 0.03e for the complexes. This quantity is much smaller than the charge transfer amount of the triel bond formed by Csp^n-F.[69] For three types of C hybridizations, AIM parameters suggest that the GeH_3F species is the strongest, followed by the Si and C, which corresponds to their Lewis acid strength.

The F atom has been considered as the nucleophilic source of electron density in triel bonds in the recent study.[69] However, the pertinent F was not bonded to C in the triel bond. Nonetheless, this previous study can provide enlightenment for the results shown here. For example, the Csp^n-F and TrR_3 (Tr═B, Al, Ga) complex is held together by a pair of triel bonds. The interaction energy of the complex varies from −0.94 to −29.74 kcal/mol at the MP2/aug-cc-pVTZ level.[69] The sp^3 hybridization has a stronger effect than sp^2 and sp, and the interaction energy is decreased in the order of sp^3 < sp^2 < sp.[69]

5. CONCLUSIONS

The tetrel-bonded complexes between the organic halogen connected with differently hybridized C atoms and TH_3F (T═C, Si, Ge) have been investigated by *ab initio* calculations. The strength of the tetrel bond is related to the C hybridization as well as the nature of both X and T. For any type of C hybridization, the GeH_3F complexes are more strongly bound than the SiH_3F analogues, which are stronger than the CH_3F analogues. For T═C complexes, the interaction energy shows a similar increasing tendency with the decrease of the electronegativity of halogen substituents. This is also same for T═Si complexes in both sp and sp^3 hybridization except for the sp^2 hybridization.

NBO analysis shows that the principal orbital interaction of these tetrel bonds is charge transfer from the lone pair on X in the Lewis base into the empty F-T orbital. Furthermore, the values are related to the type of C hybridization, with the order of sp^3 > sp^2 > sp. The bond critical point between T and X confirms the existence of the tetrel bond. For both sp and sp^3 hybridizations, the tetrel bonds are dominated by electrostatic interaction, while for the sp^2 hybridization, both electrostatic and dispersion have similar degrees of magnitude, except for the H_2C═CHF···GeH_3F complex, which means that those two terms make comparable contributions to the energetic stability of the H_2C═CHX complexes.

AUTHOR INFORMATION

Corresponding Authors

Xiaolong Zhang − *The Laboratory of Theoretical and Computational Chemistry, School of Chemistry and Chemical Engineering, Yantai University, Yantai 264005, People's Republic of China*; Phone: (+086) 535 6902063; Email: xiaolongzhang@ytu.edu.cn; Fax: (+086) 535 6902063

Qingzhong Li − *The Laboratory of Theoretical and Computational Chemistry, School of Chemistry and Chemical Engineering, Yantai University, Yantai 264005, People's Republic of China*; orcid.org/0000-0003-1486-6772; Email: lqz@ytu.edu.cn

Author

Qingqing Yang − *The Laboratory of Theoretical and Computational Chemistry, School of Chemistry and Chemical Engineering, Yantai University, Yantai 264005, People's Republic of China*

Complete contact information is available at: https://pubs.acs.org/10.1021/acsomega.1c04085

Notes

The authors declare no competing financial interest.

https://doi.org/10.1021/acsomega.1c04085
ACS Omega 2021, 6, 29037−29044

■ ACKNOWLEDGMENTS

This work was supported by the National Natural Science Foundation of China (21573188).

■ REFERENCES

(1) Bauzá, A.; Mooibroek, T. J.; Frontera, A. Tetrel-bonding interaction: Rediscovered supramolecular force? *Angew. Chem., Int. Ed.* **2013**, *52*, 12317−12321.
(2) Clark, T.; Hennemann, M.; Murray, J. S.; Politzer, P. Halogen bonding: The σ-hole. *J. Mol. Model.* **2007**, *13*, 291−296.
(3) Murray, J. S.; Lane, P.; Politzer, P. Expansion of the σ-hole concept. *J. Mol. Model.* **2009**, *15*, 723−729.
(4) Murray, J. S.; Lane, P.; Clark, T.; Riley, K. E.; Politzer, P. σ-Holes, π-holes and electrostatically-driven interactions. *J. Mol. Model.* **2012**, *18*, 541−548.
(5) Grabowski, S. J. Tetrel bond−σ-hole bond as a preliminary stage of the S_N2 reaction. *Phys. Chem. Chem. Phys.* **2014**, *16*, 1824−1834.
(6) Bauzá, A.; Seth, S. K.; Frontera, A. Tetrel bonding interactions at work: Impact on tin and lead coordination compounds. *Coord. Chem. Rev.* **2019**, *384*, 107−125.
(7) Mirdya, S.; Roy, S.; Chatterjee, S.; Bauzá, A.; Frontera, A.; Chattopadhyay, S. Importance of π-interactions involving chelate rings in addition to the tetrel bonds in crystal engineering: A combined experimental and theoretical study on a series of hemi-and holodirected nickel (II)/lead (II) complexes. *Cryst. Growth Des.* **2019**, *19*, 5869−5881.
(8) Frontera, A.; Bauzá, A. S···Sn tetrel bonds in the activation of peroxisome proliferator-activated receptors (PPARs) by organotin molecules. *Chem. − Eur. J.* **2018**, *24*, 16582−16587.
(9) Liu, M.; Li, Q.; Cheng, J.; Li, W.; Li, H.-B. Tetrel bond of pseudohalide anions with XH_3F (X═C, Si, Ge, and Sn) and its role in S_N2 reaction. *J. Chem. Phys.* **2016**, *145*, 224310.
(10) Scheiner, S. Tetrel bonding as a vehicle for strong and selective anion binding. *Molecules* **2018**, *23*, 1147.
(11) Scheiner, S. Assembly of effective halide receptors from components. Comparing hydrogen, halogen, and tetrel bonds. *J. Phys. Chem. A* **2017**, *121*, 3606−3615.
(12) Bauzá, A.; Ramis, R.; Frontera, A. Computational study of anion recognition based on tetrel and hydrogen bonding interaction by calix[4]pyrrole derivatives. *Comput. Theor. Chem.* **2014**, *1038*, 67−70.
(13) García-LLinás, X.; Bauzá, A.; Seth, S. K.; Frontera, A. Importance of R−CF_3···O tetrel bonding interactions in biological systems. *J. Phys. Chem. A* **2017**, *121*, 5371−5376.
(14) Montaña, Á. M. The σ and π-holes. The halogen and tetrel bondings: Their nature, importance and chemical, biological and medicinal implications. *ChemistrySelect* **2017**, *2*, 9094−9112.
(15) Bauzá, A.; Frontera, A. RCH_3···O interactions in biological systems: Are they trifurcated H-bonds or noncovalent carbon bonds? *Crystals* **2016**, *6*, 26.
(16) Scheiner, S. Systematic elucidation of factors that influence the strength of tetrel bonds. *J. Phys. Chem. A* **2017**, *121*, 5561−5568.
(17) Dong, W.; Li, Q.; Scheiner, S. Comparative strengths of tetrel, pnicogen, chalcogen, and halogen bonds and contributing factors. *Molecules* **2018**, *23*, 1681.
(18) Hou, M. C.; Yang, S. B.; Li, Q. Z.; Cheng, J. B.; Li, H. B.; Liu, S. F. Tetrel bond between 6-OTX_3-fulvene and NH_3, substituents and aromaticity. *Molecules* **2019**, *24*, 10.
(19) Wei, Y. X.; Li, H. B.; Cheng, J. B.; Li, W. Z.; Li, Q. Z. Prominent enhancing effects of substituents on the strength of π···σ-hole tetrel bond. *Int. J. Quantum Chem.* **2017**, *117*, No. e25448.
(20) Del Bene, J. E.; Alkorta, I.; Elguero, J. Exploring N···C tetrel and O···S chalcogen bonds in HN(CH)SX: OCS systems, for X= F, NC, Cl, CN, CCH, and H. *Chem. Phys. Lett.* **2019**, *730*, 466−471.
(21) Xu, H.; Cheng, J.; Yu, X.; Li, Q. Abnormal tetrel bonds between formamidine and TH_3F: substituent effects. *ChemistrySelect* **2018**, *3*, 2842−2849.
(22) Guo, X.; Liu, Y. W.; Li, Q. Z.; Li, W. Z.; Cheng, J. B. Competition and cooperativity between tetrel bond and chalcogen bond in complexes involving F_2CX (X= Se and Te). *Chem. Phys. Lett.* **2015**, *620*, 7−12.
(23) Scheiner, S. Steric crowding in tetrel bonds. *J. Phys. Chem. A* **2018**, *122*, 2550−2562.
(24) Hou, M.; Zhu, Y.; Li, Q.; Scheiner, S. Tuning the competition between hydrogen and tetrel bonds by a magnesium bond. *ChemPhysChem* **2020**, *21*, 212−219.
(25) Alkorta, I.; Montero-Campillo, M. M.; Mó, O.; Elguero, J.; Yáñez, M. Weak interactions get strong: Synergy between tetrel and alkaline-earth bonds. *J. Phys. Chem. A* **2019**, *123*, 7124−7132.
(26) Marín-Luna, M.; Alkorta, I.; Elguero, J. Cooperativity in tetrel bonds. *J. Phys. Chem. A* **2016**, *120*, 648−656.
(27) Mahmoudi, G.; Bauzá, A.; Amini, M.; Molins, E.; Mague, J. T.; Frontera, A. On the importance of tetrel bonding interactions in lead (II) complexes with (iso) nicotinohydrazide based ligands and several anions. *Dalton Trans.* **2016**, *45*, 10708−10716.
(28) Hussain, M.; Bauzá, A.; Frontera, A.; Lo, K. M.; Naseer, M. M. Structure guided or structure guiding? Mixed carbon/hydrogen bonding in a bis-Schiff base of N-allyl isatin. *CrystEngComm* **2018**, *20*, 150−154.
(29) Shukla, R.; Chopra, D. Characterization of the short O=C···O=C π-hole tetrel bond in the solid state. *CrystEngComm* **2018**, *20*, 3308−3312.
(30) Mahmoudi, G.; Bauzá, A.; Frontera, A. Concurrent agostic and tetrel bonding interactions in lead (II) complexes with an isonicotinohydrazide based ligand and several anions. *Dalton Trans.* **2016**, *45*, 4965−4969.
(31) Esrafili, M. D.; Mohammadirad, N.; Solimannejad, M. Tetrel bond cooperativity in open-chain $(CH_3CN)_n$ and $(CH_3NC)_n$ clusters (n=2-7): An ab initio study. *Chem. Phys. Lett.* **2015**, *628*, 16−20.
(32) Esrafili, M. D.; Mohammadian-Sabet, F. Cooperativity of tetrel bonds tuned by substituent effects. *Mol. Phys.* **2016**, *114*, 1528−1538.
(33) Esrafili, M. D.; Asadollahi, S.; Mousavian, P. Anionic tetrel bonds: An ab initio study. *Chem. Phys. Lett.* **2018**, *691*, 394−400.
(34) Mani, D.; Arunan, E. The X−C···π (X= F, Cl, Br, Cn) carbon bond. *J. Phys. Chem. A* **2014**, *118*, 10081−10089.
(35) Li, Q. Z.; Zhuo, H. Y.; Li, H. B.; Liu, Z. B.; Li, W. Z.; Cheng, J. B. Tetrel-hydride interaction between XH_3F(X= C, Si, Ge, Sn) and HM (M-Li, Na, BeH, MgH). *J. Phys. Chem. A* **2015**, *119*, 2217−2224.
(36) Li, Q.; Guo, X.; Yang, X.; Li, W.; Cheng, J.; Li, H.-B. A σ-hole interaction with radical species as electron donors: Does single-electron tetrel bonding exist? *Phys. Chem. Chem. Phys.* **2014**, *16*, 11617−11625.
(37) Liu, M.; Li, Q.; Li, W.; Cheng, J. Carbene tetrel-bonded complexes. *Struct. Chem.* **2017**, *28*, 823−831.
(38) Donald, K. J.; Tawfik, M. The weak helps the strong: Sigma-holes and the stability of MF_4·base complexes. *J. Phys. Chem. A* **2013**, *117*, 14176−14183.
(39) Xu, H.; Cheng, J.; Yang, X.; Liu, Z.; Li, W.; Li, Q. Comparison of σ-hole and π-hole tetrel bonds formed by pyrazine and 1, 4-dicyanobenzene: The interplay between anion-π and tetrel bonds. *ChemPhysChem* **2017**, *18*, 2442−2450.
(40) Liu, M.; Li, Q.; Li, W.; Cheng, J. Tetrel bonds between $PySiX_3$ and some nitrogenated bases: Hybridization, substitution, and cooperativity. *J. Mol. Graphics Modell.* **2016**, *65*, 35−42.
(41) Politzer, P.; Murray, J. S.; Lane, P.; Concha, M. C. Electrostatically driven complexes of SiF_4 with amines. *Int. J. Quantum Chem.* **2009**, *109*, 3773−3780.
(42) Bauzá, A.; Mooibroek, T. J.; Frontera, A. Small cycloalkane $(CN)_2CC(CN)_2$ structures are highly directional non-covalent carbon-bond donors. *Chem. − Eur. J.* **2014**, *20*, 10245−10248.
(43) Southern, S. A.; Bryce, D. L. NMR investigations of noncovalent carbon tetrel bonds. Computational assessment and initial experimental observation. *J. Phys. Chem. A* **2015**, *119*, 11891−11899.

https://doi.org/10.1021/acsomega.1c04085
ACS Omega 2021, 6, 29037−29044

(44) De, V.; Nziko, P. N.; Scheiner, S. Comparison of π-hole tetrel bonding with σ-hole halogen bonds in complexes of XCN (X= F, Cl, Br, I) and NH_3. *Phys. Chem. Chem. Phys.* **2016**, *18*, 3581−3590.
(45) Alkorta, I.; Elguero, J.; Del Bene, J. E. Azines as electron-pair donors to CO_2 for N···C tetrel bonds. *J. Phys. Chem. A* **2017**, *121*, 8017−8025.
(46) Wei, Y.; Li, Q.; Scheiner, S. Pi tetrel bonds, and their influence on hydrogen bonds and proton transfers. *ChemPhysChem* **2018**, *19*, 736−743.
(47) Chandra, S.; Bhattacharya, A. Attochemistry of ionized halogen, chalcogen, pnicogen, and tetrel noncovalent bonded clusters. *J. Phys. Chem. A* **2016**, *120*, 10057−10071.
(48) Zierkiewicz, W.; Michalczyk, M.; Scheiner, S. Implications of monomer deformation for tetrel and pnicogen bonds. *Phys. Chem. Chem. Phys.* **2018**, *20*, 8832−8841.
(49) Liu, M. X.; Li, Q. Z.; Scheiner, S. Comparison of tetrel bonds in neutral and protonated complexes of pyridineTF_3 and furanTF_3 (T= C, Si, and Ge) with NH_3. *Phys. Chem. Chem. Phys.* **2017**, *19*, 5550−5559.
(50) Xu, H.-L.; Cheng, J.-B.; Li, H.-B.; Yang, X.; Liu, Z.-B.; Xiao, B.; Li, Q.-Z. Tetrel bonds between $PhSiF_3$/$PhTH_3$ (T = Si, Ge, Sn) and H_3ZO (Z = N, P, As): A pentacoordinate silicon (IV) complex. *Int. J. Quant. Chem.* **2018**, *118*, No. e25660.
(51) Dong, W.; Niu, B.; Liu, S.; Cheng, J.; Liu, S.; Li, Q. Comparison of σ−/π-hole tetrel bonds between TH_3F/F_2TO and H_2CX (X=O, S, Se). *ChemPhysChem* **2019**, *20*, 627−635.
(52) Scheiner, S. Highly selective halide receptors based on chalcogen, pnicogen, and tetrel bonds. *Chem. − Eur. J.* **2016**, *22*, 18850−18858.
(53) Scheiner, S. Comparison of halide receptors based on H, halogen, chalcogen, pnicogen, and tetrel bonds. *Faraday Discuss.* **2017**, *203*, 213−226.
(54) Esrafili, M. D.; Mousavian, P. Strong tetrel bonds: Theoretical aspects and experimental evidence. *Molecules* **2018**, *23*, 2642.
(55) Mani, D.; Arunan, E. The X−C···Y (X= O /F, Y= O/ S/ F/ Cl/ Br /N /P) 'carbon bond' and hydrophobic interactions. *Phys. Chem. Chem. Phys.* **2013**, *15*, 14377−14383.
(56) Liu, M.; Li, Q.; Li, W.; Cheng, J.; McDowell, S. A. C. Comparison of hydrogen, halogen, and tetrel bonds in the complexes of HArF with YH_3X (X= halogen, Y=C and Si). *RSC Adv.* **2016**, *6*, 19136−19143.
(57) Legon, A. C. Tetrel, pnictogen and chalcogen bonds identified in the gas phase before they had names: A systematic look at non-covalent interactions. *Phys. Chem. Chem. Phys.* **2017**, *19*, 14884−14896.
(58) Alkorta, I.; Rozas, I.; Elguero, J. Molecular complexes between silicon derivatives and electron-rich groups. *J. Phys. Chem. A* **2001**, *105*, 743−749.
(59) Berger, R.; Resnati, G.; Metrangolo, P.; Weberd, E.; Hulliger, J. Organic fluorine compounds: A great opportunity for enhanced materials properties. *Chem. Soc. Rev.* **2011**, *40*, 3496−3508.
(60) Borisenko, K. B.; Gould, R. O.; Morrison, C. A.; Parsons, S.; Rankin, D. W. H. A theoretical and experimental study of weak silane−electron donor interactions. *J. Mol. Struct.* **2000**, *554*, 163−172.
(61) Cormanich, R. A.; Rittner, R.; Hagan, D. O.; Bühl, M. Inter-and intramolecular CF···CO interactions on aliphatic and cyclohexane carbonyl derivatives. *J. Comput. Chem.* **2016**, *37*, 25−33.
(62) Boys, S. F.; Bernardi, F. The calculation of small molecular interactions by the differences of separate total energies. Some procedures with reduced errors. *Mol. Phys.* **1970**, *19*, 553−566.
(63) Frisch, M. J.; Trucks, G. W.; Schlegel, H. B.; Scuseria, G. E.; Robb, M. A.; Cheeseman, J. R.; Scalmani, G.; Barrone, V.; Mennucci, B.; Petersson, G.A. et al. *Gaussian 09*; Revision A.02, Gaussian, Inc.: Wallingford, 2009.
(64) Bulat, F. A.; Toro-Labbé, A.; Brinck, T.; Murray, J. S.; Politzer, P. Quantitative analysis of molecular surfaces: Areas, volumes, electrostatic potentials and average local ionization energies. *J. Mol. Model.* **2010**, *16*, 1679−1691.
(65) Reed, A. E.; Curtiss, L. A.; Weinhold, F. Intermolecular interactions from a natural bond orbital, donor-acceptor viewpoint. *Chem. Rev.* **1988**, *88*, 899−926.
(66) Bader, R. F. W. *AIM2000 Program*; V.2.0 McMaster University: Hamilton, Canada, 2000
(67) Su, P.; Li, H. Energy decomposition analysis of covalent bonds and intermolecular interactions. *J. Chem. Phys.* **2009**, *131*, No. 014102.
(68) Schmidt, M. W.; Baldridge, K. K.; Boatz, J. A.; Elbert, S. T.; Gordon, M. S.; Jensen, J. H.; Koseki, S.; Matsunaga, N.; Nguyen, K. A.; Su, S.; Windus, T. L.; Dupuis, M.; Montgomery, J. A., Jr. General atomic and molecular electronic structure system. *J. Comput. Chem.* **1993**, *14*, 1347−1363.
(69) Yang, Q.; Chi, Z.; Li, Q.; Steve, S. Effect of carbon hybridization in C-F bond as an electron donor in triel bonds. *J. Chem. Phys.* **2020**, *153*, No. 074304.

https://doi.org/10.1021/acsomega.1c04085
ACS Omega 2021, 6, 29037−29044